Role of Carbonic Anhydrase IV in Corneal Endothelial HCO_3^- Transport

Xing Cai Sun, Jinhua Li, Miao Cui, and Joseph A. Bonanno

Purpose. Carbonic anhydrase activity has a central role in corneal endothelial function. The authors examined the role of carbonic anhydrase IV (CAIV) in facilitating CO_2 flux, HCO_3^- permeability, and HCO_3^- flux across the apical membrane.

Methods. Primary cultures of bovine corneal endothelial cells were established on membrane-permeable filters. Apical CAIV was inhibited by benzolamide or siRNA knockdown of CAIV. Apical CO_2 fluxes and HCO_3^- permeability were determined by measuring pH_i changes in response to altering the CO_2 or HCO_3^- gradient across the apical membrane. Basolateral to apical (B-to-A) HCO_3^- flux was determined by measuring the pH of a weakly buffered apical bath in the presence of basolateral bicarbonate-rich Ringer solution. In addition, the effects of benzolamide and CAIV knockdown on steady state ΔpH (apical-basolateral compartment pH) after 4-hour incubation in DMEM were measured.

Results. CAIV expression was confirmed, and CAIV was localized exclusively to the apical membrane by confocal microscopy. Both 10 μM benzolamide and CAIV siRNA reduced apparent apical CO_2 flux by approximately 20%; however, they had no effect on HCO_3^- permeability or HCO_3^- flux. The steady state apical-basolateral pH gradient at 4 hours was reduced by 0.12 and 0.09 pH units in benzolamide- and siRNA-treated cells, respectively, inconsistent with a net cell-to-apical compartment CO_2 flux.

Conclusions. CAIV does not facilitate steady state cell-to-apical CO_2 flux, apical HCO_3^- permeability, or B-to-A HCO_3^- flux. Steady state pH changes, however, suggest that CAIV may have a role in buffering the apical surface. (*Invest Ophthalmol Vis Sci.* 2008;49:1048–1055) DOI:10.1167/iovs.07-1188

Carbonic anhydrase activity has a central role in corneal endothelial function. Several laboratories[1–4] have consistently shown that rabbit corneas mounted in vitro in a Dikstein-Maurice–type chamber swell in response to direct application of carbonic anhydrase inhibitors (CAIs) to the endothelial surface. Clinically, topical use of CAIs generally does not affect normal corneas, presumably because of the much lower concentration of drug at the endothelial surface.[5–9] However, topical CAIs can cause corneal edema in corneas with low endothelial cell density,[10,11] suggesting that there is a threshold reserve of carbonic anhydrase activity or that inhibition of CA activity has a greater impact when other endothelial properties (e.g., barrier function) are compromised. At least two CA isoforms are expressed in corneal endothelium, the cytosolic CAII[12–14] and the membrane-bound CAIV.[15–17] SAGE analysis suggests that another membrane isoform, CAXII, is also expressed.[18]

The sensitivity of corneal endothelial fluid transport to CAIs and the abrogation of fluid transport in the absence of HCO_3^-[1,2,19] have led to the notion that endothelial fluid transport is caused by transport of HCO_3^- that is facilitated by CA activity. All carbonic anhydrases significantly speed the hydration and dehydration of CO_2. At membrane interfaces, CA activity can facilitate net CO_2 flux[20] and transport of HCO_3^-.[21,22] Recent studies have suggested that HCO_3^- transporters can form complexes with CAII or CAIV (transport metabolons) and can facilitate HCO_3^- fluxes by rapid conversion to CO_2, thereby maximizing local HCO_3^- gradients.[23–25] CAIs also produce acidosis consistent with their contribution to HCO_3^- buffering capacity.[26,27] In corneal endothelium, the application of acetazolamide, a cell-permeant CAI, reduces intracellular pH (pH_i).[28] The mechanism(s) by which CA activity contributes to corneal endothelial function by facilitating CO_2 flux, HCO_3^- flux, or buffering capacity, however, is unknown.

Most readily available CAIs are cell permeant and inhibit all CA isoforms. One recent study,[29] however, has shown that the relatively impermeant CAI, benzolamide, and a dextran-linked CAI can cause swelling of rabbit corneas in vitro at about half the rate of cell-permeant CAIs, indicating that CAIV and CAII have additive functions. Benzolamide applied to the apical surfaces of corneal endothelial cells can slow apical CO_2 fluxes; this process is reversed by the addition of CA to the bath.[30] These results suggested that CO_2 diffusion from cell-to-apical surface, followed by conversion to HCO_3^- (facilitated by CAIV), may contribute to net HCO_3^- transport, but they do not show that this process actually occurs.

In this study, we examined the role of CAIV in apical CO_2 flux, apical HCO_3^- permeability, basolateral-to-apical HCO_3^- flux, and steady state bath pH changes across cultured bovine corneal endothelium by comparison of these parameters with benzolamide or CAIV siRNA-treated monolayers. The results indicated that CAIV does not have a role in net CO_2 flux, apical HCO_3^- permeability, or HCO_3^- flux and suggested that CAIV may function to buffer the apical surface.

Materials and Methods

Cell Culture

Bovine corneal endothelial cells (BCECs) were cultured to confluence onto 25-mm round coverslips, 13-mm filters (Anodisc; Whatman, Maidstone, Kent, UK), tissue culture inserts (Anopore; Whatman), or T-25 flasks, as described.[31] Briefly, primary cultures from fresh cow eyes were established in T-25 flasks with 3 mL Dulbecco modified Eagle medium (DMEM), 10% bovine calf serum, and antibiotic (penicillin 100 U/mL, streptomycin 100 U/mL, and fungizone 0.25 μg/mL), gassed with 5% CO_2-95% air at 37°C, and fed every 2 to 3 days. Primary cultures were subcultured to three T-25 flasks and grown to confluence in 3 to 5 days. Resultant second-passage cultures were then further subcultured onto coverslips, filters (Anodisc; Whatman), or

From Indiana University, School of Optometry, Bloomington, Indiana.

Supported by National Institutes of Health Grant EY08834.

Submitted for publication September 11, 2007; revised October 11 and October 29, 2007; accepted December 19, 2007.

Disclosure: **X.C. Sun**, None; **J. Li**, None; **M. Cui**, None; **J.A. Bonanno**, None

The publication costs of this article were defrayed in part by page charge payment. This article must therefore be marked "*advertisement*" in accordance with 18 U.S.C. §1734 solely to indicate this fact.

Corresponding author: Joseph A. Bonanno, Indiana University, School of Optometry, 800 E. Atwater Avenue, Bloomington, IN 47405; jbonanno@indiana.edu.

tissue culture inserts (Anopore; Whatman) and allowed to reach confluence within 5 to 7 days.

RT-PCR Screening

mRNA was extracted and purified from fresh and cultured BCECs and from bovine lung using the mRNA mini-kit (Oligotex; Qiagen, Valencia, CA) according to the manufacturer's protocol. Purified mRNA was then used for cDNA synthesis and CAIV PCR. cDNA synthesis was performed using reverse transcriptase (Superscript III; 200 U/μL; Invitrogen, Carlsbad, CA), Oligo dT_{12-18} primer, and 1 μg mRNA, as previously described.[32] PCR was performed with 100 μL CAIV in a PCR reaction buffer (Expand High Fidelity; Roche, Basel, Switzerland) with 0.5 μL *Taq* polymerase (Roche), 5 μL cDNA template, 8 μL dNTP mix (2.5 mM each), and 0.3 μM (final concentration) CAIV primers. PCR parameters were denaturation at 94°C for 3 minutes for one cycle, 30 cycles of denaturation at 94°C for 30 seconds each, annealing at 50°C to 60°C for 1 minute, extension at 71°C for 2 minutes, and a final extension for one cycle at 71°C for 10 minutes. PCR products were separated on 1.7% agarose electrophoresis gels and stained with 0.5 μg/mL ethidium bromide. Water and no-RT controls were routinely added. CAIV primers were product length, 468 bp; CAIV sense, 5′-TGCTACCAGATTCAAGTCAAGCCTTC-3′; and CAIV antisense, 5′-AAGTTCACATTCTTGGATCCGTCCAC-3′. Expected PCR bands were excised from the agarose gel, purified using a gel purification kit (Qiagen), subcloned into pCR-TOPO downstream from a T7 sequence, and transformed into *Escherichia coli* (One Shot Chemically Competent; Invitrogen). This plasmid was submitted to the Biochemistry Biotechnology Facility at Indiana University School of Medicine, Indianapolis, for sequencing. Confirmation of our PCR results was obtained by comparison of the sequence results using BLAST software (National Center for Biotechnology Information [NCBI]) against the NCBI database.

siRNA Transfection

siRNA construction and treatment were performed as described.[32–35] Briefly, several sense and antisense sequences corresponding to CAIV cDNA were designed and blasted by using the siRNA targeting design tool (Ambion, Austin, TX) and were purchased from Invitrogen. Using these oligonucleotides, four 21-nucleotide siRNAs for CAIV were synthesized using the siRNA construction kit (Silencer) from Ambion. We found that 20 nM target sequence 120–140 of the CAIV open reading frame 5′-AAGTCAAGCCTTCCAACTACA-3′ antisense and 5′-AATGTAGTTGGAAGGCTTGAC sense was most effective 3 to 4 days after transfection. Nontargeting siRNA (siCONTROL; no known mammalian homology) was purchased from Dharmacon (Chicago, IL). When cells were 70% to 80% confluent, they were transfected (Oligofectamine; Invitrogen) in accordance with the manufacturer's protocol and in the presence of siRNA. Cells were incubated for 4 hours in medium (1 mL OPTI-MEM I; Gibco, Grand Island, NY) containing siRNA; this was followed by the addition of 2 mL standard DMEM with serum. T-25 flasks were treated with 2 mL medium (OPTI-MEM I; Gibco) containing siRNA, followed by the addition of 4 mL culture media. Media were then changed every 2 days.

Immunoblotting

Total membrane protein was extracted from fresh and cultured BCECs using the sulfo-NHS-biotin technique, as described.[36] Cultured and fresh bovine corneal endothelial surface proteins were labeled with 200 μg EZ-link sulfo-NHS-biotin (Pierce) per milliliter of bicarbonate-free Ringer solution, pH 7.5, at room temperature for 30 minutes. Cells were lysed (50 mM Tris base, 150 mM NaCl, 0.5% deoxycholic acid-sodium salt, 2% SDS, and 1% NP-40, pH 7.5, protease inhibitor cocktail) and then sonicated. This was followed by centrifugation at 10,000 rpm to pellet cell debris. The supernatant was incubated with 50 μL immobilized streptavidin at 4°C for overnight, rotated end over end. The streptavidin-biotinylated protein complex was pelleted at 10,000 rpm for 5 minutes and washed four times. Fifty microliters of 1× Laemmli sample buffer was then added, and the mixture was heated in a 95°C heating block for 10 minutes to denature the protein and break the streptavidin-biotinylated protein bond. Streptavidin beads were pelleted on a table-top microcentrifuge, and the supernatant was quickly removed. An aliquot of the supernatant was taken for protein concentration measurement according to the Bradford assay (Bio-Rad, Hercules, CA). Thirty-microgram samples were resolved on SDS-PAGE and transferred to a polyvinylidene difluoride membrane (Bio-Rad). Blots were then probed with CAIV polyclonal antibody (a kind gift from W. Sly; 1:2000), and bound antibody was detected using enhanced chemiluminescence. The membrane was then stripped with strong antibody stripping solution (Reblot Plus; Chemicon, Temecula, CA) to remove CAIV antibody. Blots were incubated with β-actin polyclonal antibody (Sigma; 1:10,000) and developed by enhanced chemiluminescence. Films were scanned to produce digital images that were then assembled and labeled using graphics editing software (Photoshop; Adobe, San Jose, CA).

Immunofluorescence

Cultured cells grown to confluence on coverslips were washed three to four times with warmed (37°C) PBS and fixed for 30 minutes in warmed PLP fixation solution (2% paraformaldehyde, 75 mM lysine, 10 mM sodium periodate, and 45 mM sodium phosphate, pH 7.4) on a rocker. After fixation, the cells were washed three to four times with PBS. Cells were blocked for 1 hour in PBS that contained 0.2% saponin, bovine serum albumin, 5% goat serum, 0.01% saponin, and 50 mM NH_4Cl. Rabbit polyclonal CAIV antibody and rat monoclonal ZO-1 antibody (mAb1520; Chemicon), diluted 1:100 together in PBS/goat serum (1:1), were added onto coverslips and incubated for 1 hour at room temperature or overnight at 4°C. Coverslips were washed three times for 15 minutes in PBS that contained 0.01% saponin. Secondary antibodies conjugated to fluorescent dyes (Alexa 488 [NBC1], 1:1000; Alexa Fluor 594 [ZO-1], 1:1000; Molecular Probes) were applied for 1 hour at room temperature. Coverslips were washed with water and mounted with antifade medium (Prolong; Molecular Probes) according to the manufacturer's instructions. Immunostaining was observed with a 40× oil objective lens using a standard epifluorescence microscope equipped with a charge-coupled device camera. A laser scanning confocal microscope (Bio-Rad 2000; Bio-Rad) was used to obtain image stacks at 0.5-μm separation. Montages were created with image acquisition and analysis software (Metamorph; Universal Imaging, West Chester, PA).

Microscope Perfusion

For measurement of CO_2 and HCO_3^- transendothelial flux, cells were cultured to confluence on 13-mm diameter, 0.2-μm membrane filters (Anodisc; Whatman) placed in a double-sided perfusion chamber designed for independent perfusion of the apical and basolateral sides.[37] The assembled chamber was placed on a water-jacketed (37°C) brass collar held on the stage of an inverted microscope (Diaphot 200; Nikon, Tokyo, Japan) and viewed with a long working distance (2 mm) water-immersion objective (40×; Nikon). Apical and basolateral compartments were connected to hanging syringes that contained Ringer solution in a polymethyl methacrylate (Plexiglas; Altuglas, Philadelphia, PA) warming box (37°C) with tubing (Phar-Med; Saint-Gobain Performance Plastics, Paris, France). The flow of the perfusate (approximately 0.5 mL/min) was achieved by gravity. Two independent eight-way valves were used to select the desired perfusate for the apical and basolateral chambers. The composition of the standard HCO_3^--rich Ringer solution used throughout the study was 150 mM Na^+, 4 mM K^+, 0.6 mM Mg^{2+}, 1.4 mM Ca^{2+}, 118 mM Cl^-, 1 mM HPO_4^-, 10 mM $HEPES^-$, 28.5 mM HCO_3^-, 2 mM $gluconate^-$, and 5 mM glucose, equilibrated with 5% CO_2 and pH adjusted to 7.50 at 37°C. HCO_3^--free Ringer solution (pH 7.50) was prepared by equimolar substitution of $NaHCO_3$ with sodium gluconate. Low-HCO_3^- Ringer solution (2.85 mM HCO_3^-, pH 6.5) was prepared by replacing 25.65 mM $NaHCO_3$ with sodium gluconate.

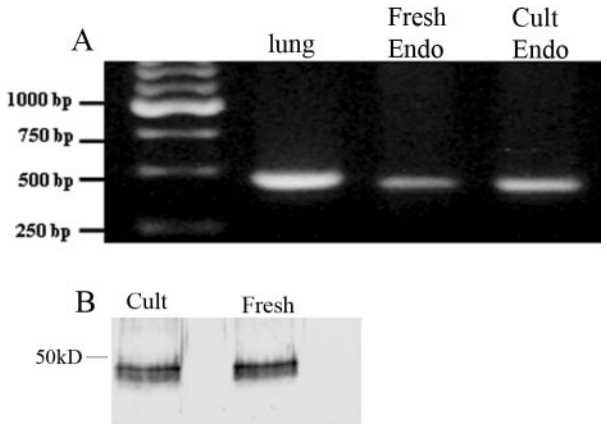

FIGURE 1. (**A**) RT-PCR result for CAIV from bovine lung (positive control), fresh bovine corneal endothelium, and cultured bovine corneal endothelium. (**B**) Western blot of membrane preparations from cultured and fresh bovine corneal endothelium.

Measurement of Apparent CO_2 Flux

Apparent CO_2 flux was measured as described.[33] BCECs cultured onto permeable filters (Anodisc; Whatman) were loaded with the pH-sensitive fluorescent dye BCECF. Intracellular pH (pH_i) was measured by obtaining fluorescence ratios (495 and 440 nM) of BCECF-loaded cells at 1 second^{-1}. CO_2 flux from cell to apical compartment was determined using a constant pH protocol, as described.[30,33] Briefly, in the constant pH protocol, the HCO_3^--rich Ringer solution on the apical side is replaced with a CO_2 and HCO_3^--free Ringer solution of the same pH (HEPES buffered). Under this protocol, the initial pHi change is caused by rapid CO_2 efflux (increase in pHi). The maximum slope of the pHi decrease is taken as an estimate of CO_2 flux.

Measurement of HCO_3^- Permeability

HCO_3^- permeability of the apical membrane was determined using a constant CO_2 protocol, as described.[33] Under the constant CO_2 protocol, the HCO_3^--rich ringer (28.5 mM, 5% CO_2, pH 7.5) is replaced with a low HCO_3^- (LB) solution (2.85 mM, 5% CO_2, pH 6.5). Under this protocol the initial pHi change is predominantly caused by HCO_3^- efflux because there is no CO_2 gradient. However, there is a pH gradient that can contribute (approximately 15%) to the initial pHi decrease.[30]

Measurement of Transendothelial HCO_3^- Flux

Transendothelial HCO_3^- flux was measured as described.[33] Briefly, BCECs cultured onto permeable filters (Anodisc; Whatman), perfused in a double-side chamber, were exposed to the standard HCO_3^--rich solution (5% CO_2/28.5 mM HCO_3^-, pH 7.5) on the basolateral and apical sides at 37°C. A low HCO_3^- solution (5% CO_2/2.85 mM HCO_3^-, pH 6.5), without HEPES buffer and containing 1 μM BCECF-free acid, was then quickly exchanged on the apical side of the chamber, and the exit tube on that side was clamped. The pH of the low HCO_3^- solution was estimated (1 Hz) at approximately 200 μm from the surface of the cells by measuring the fluorescence ratio of BCECF using the microscope fluorometer. The pH of the low HCO_3^- solution rose from 6.5, and the initial rate of change over the first 20 seconds after clamping was estimated and served as an indirect measure of basolateral-to-apical (B-to-A) flux.

Measurement of Steady State ΔpH

Steady state ΔpH was measured as described,[33] with minor modification. BCECs cultured to confluence on 0.2-μm membrane tissue culture inserts (Anopore; Whatman) were washed with DMEM containing 2% bovine calf serum. Two hundred microliters of this culture medium containing 1 μM BCECF-free acid was placed on the apical side, and 300 μL was placed on the basolateral side. After 4 hours in a standard 5% CO_2 incubator at 37°C, cultures were placed in a large glove box equilibrated with 5% CO_2 at 37°C. Fifty-microliter samples were taken from the apical and basolateral sides in separate glass capillary tubes, and both ends were sealed with wax. The tubes were then taken to the microscope fluorometer, and the fluorescence ratio of BCECF was measured. The pH of each sample was then determined using a standard curve constructed with solutions of known pH that had been placed within capillary tubes. The difference in pH was calculated as follows: ΔpH = apical pH − basolateral pH. A positive ΔpH indicated relative apical alkalinization.

RESULTS

Data shown in Figure 1 confirmed the presence of CAIV in BCECs. Figure 1A shows PCR results indicating CAIV expression in bovine lung (positive control), fresh corneal endothelium, and cultured corneal endothelial cells. Figure 1B shows Western blot results using membrane preparations confirming protein expression in fresh and cultured endothelium. Molecular weight was estimated to be 35 to 40 kDa, consistent with CAIV.[38]

Indirect immunofluorescence was then performed to determine the membrane localization of CAIV. Figure 2A shows positive fluorescence for CAIV that is spread across the cell surface, including the lateral junctions. There are also some concentrated caps of fluorescence near the cell center. This pattern of fluorescence is consistent with an apical localization. Figure 2B shows confocal fluorescence images using cells double stained for CAIV and the tight junction protein ZO-1. The CAIV fluorescence is either at the level of the ZO-1 fluorescence or more apical to ZO-1, consistent with the dome shape of endothelial cells and confirming an apical location for CAIV.

To complement the effects of the extracellular carbonic anhydrase inhibitor benzolamide, we subjected CAIV expression to knockdown using an siRNA approach. Figure 3A shows PCR results indicating significant knockdown at the mRNA level compared with control and siControl scrambled sequences. Figure 3B shows a representative Western blot from control, siRNA-, and siControl-treated cells. The bar graph

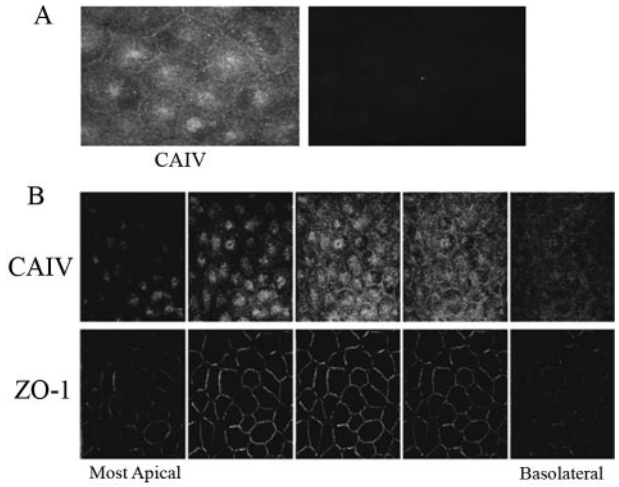

FIGURE 2. Immunofluorescence localization of CAIV in bovine corneal endothelium. (**A**) Fresh corneal endothelium. *Left*: positive surface staining. *Right*: control-absence of primary antibody. (**B**) Confocal montage of cultured corneal endothelial cells stained for CAIV and ZO-1. Leftmost image pair is the most apical section. Z-axis separation between images is 0.5 μm. The five images represent a distance of 2.5 μm. CAIV fluorescence is either apical to or coincident with ZO-1.

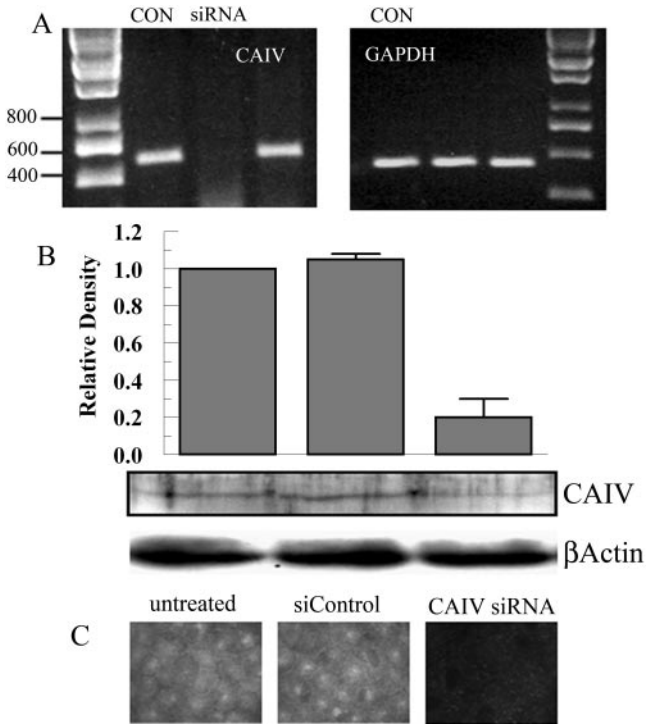

FIGURE 3. siRNA knockdown of CAIV. (**A**) Semiquantitative PCR for CAIV and GAPDH (glyceraldehyde phosphate dehydrogenase) using untreated, siRNA (20 nM)–, and siControl (20 nM)–treated cultured endothelial cells. (**B**) Western blot for CAIV and β-actin using siRNA- and siControl-treated cultured endothelial cells. Bar graph shows relative density (referenced to actin) from three paired experiments. (**C**) Immunofluorescence micrograph for CAIV.

summarizes blot densities ($n = 3$) indicating that knockdown was approximately 80%. This knockdown level is also reflected in immunofluorescence images from similarly treated cells (Fig. 3C).

Previous studies showed that 10 μM benzolamide slowed apparent CO_2 fluxes across the apical membrane by approximately 25% and that this effect could be reversed by adding carbonic anhydrase to the apical bath,[30] indicating that benzolamide inhibited an apical surface CA. Although this effect was small, it was reproducible. Furthermore, 10 μM benzolamide can cause corneal swelling,[29] so we used 10 μM benzolamide as a reference for all experiments in this study. Cells were loaded with the pH-sensitive fluorescent dye BCECF and were perfused on apical and basolateral sides with bicarbonate-rich Ringer solution. The apical perfusate was changed to bicarbonate-free Ringer solution, which induced an immediate efflux of CO_2 from the cells, causing rapid and significant cytosolic alkalinization. Figure 4A shows that 10 μM benzolamide, added to the apical side only, reduced apparent CO_2 fluxes by 23% ($n = 8$), similar to the rate previously shown.[30] To test whether CAIV knockdown by siRNA also affected apparent CO_2 flux, endothelial cells were seeded on filter (Anodisc; Whatman) membranes and treated with siRNA for CAIV or siControl. Figure 4B shows that apparent CO_2 fluxes were also reduced by 21% in CAIV siRNA-treated cells compared with siControl-treated cells. Furthermore, benzolamide had no effect on CO_2 fluxes in siRNA-treated cells (data not shown). These experiments show that apparent apical CO_2 fluxes are reduced by CAIV knockdown and are comparable to benzolamide inhibition, consistent with apparent apical CO_2 fluxes facilitated by CAIV activity.

Carbonic anhydrases, including CAIV, can form transport metabolons with bicarbonate transporters to facilitate HCO_3^- fluxes efficiently.[23,24] To determine whether this may be in place in corneal endothelium, we measured apical HCO_3^- permeability in the presence of benzolamide or using CAIV siRNA-treated cells. Cells were perfused with bicarbonate-rich Ringer solution on apical and basolateral sides. Where indicated, the apical perfusate was changed to low bicarbonate-constant CO_2 (LB) Ringer solution. Under these conditions, the change in pHi was attributed to HCO_3^- efflux and the low pH_o of the LB Ringer solution, which makes a minor contribution.[30] Figure 5 shows that neither 10 μM benzolamide nor siRNA-treated cells demonstrated a consistent inhibition of apical HCO_3^- permeability. On the other hand, 50 μM acetazolamide, which is cell permeable and blocks all CAs, reduced apparent HCO_3^- permeability by 40% (data not shown). These

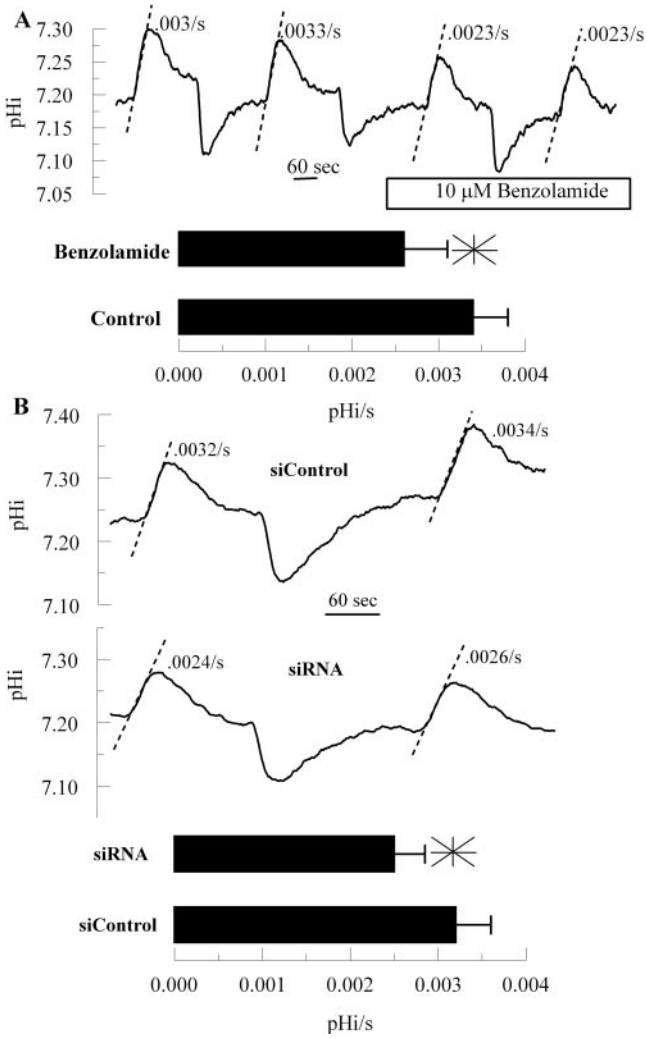

FIGURE 4. Effect of benzolamide and CAIV siRNA on apparent CO_2 fluxes. BCECF-loaded endothelial cells were perfused in a two-sided chamber. Alkalinizations were caused by changing the apical perfusate to a CO_2/HCO_3^--free Ringer solution. *Dashed lines*: estimated rate (pH_i/s). (**A**) This was performed twice in the absence and then in the presence of 10 μM benzolamide on the apical side. Bar graph shows mean rates and SD ($n = 12$ filters [Anodiscs; Whatman]). *Significantly lower than control ($P < 0.05$; paired *t*-test). (**B**) Representative comparisons of siControl- and CAIV-treated cells. Bar graph shows mean rates and SD ($n = 10$ filter [Anodiscs; Whatman]). *Significantly lower than control ($P < 0.05$; independent *t*-test).

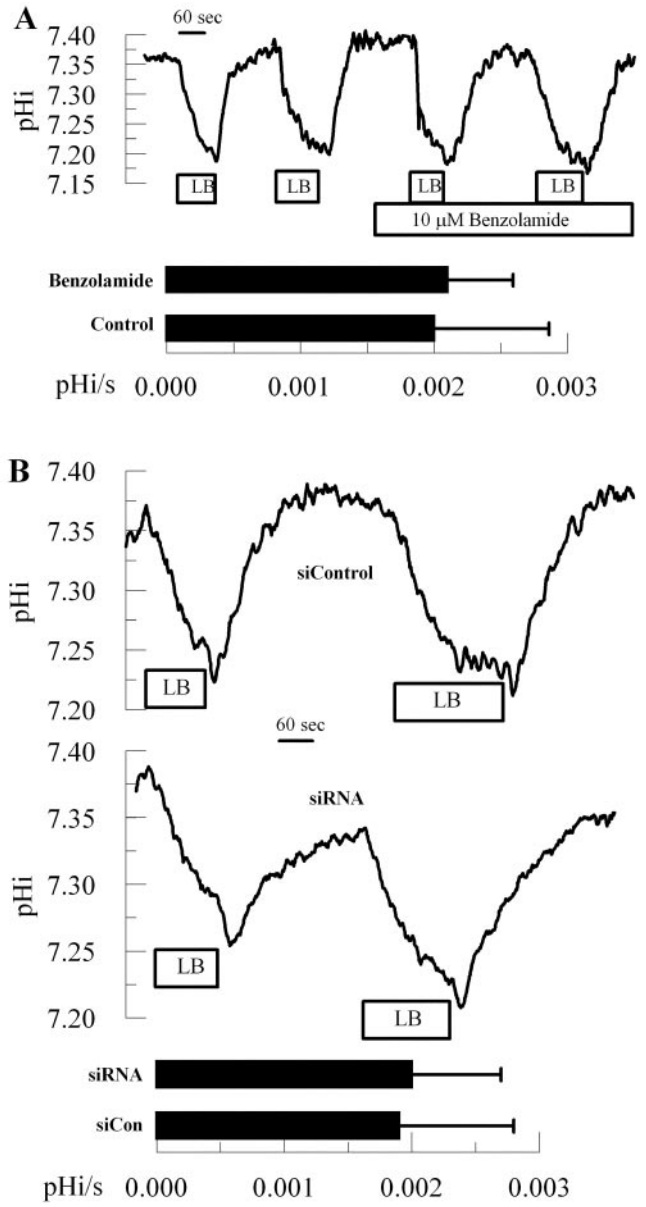

FIGURE 5. Effect of benzolamide and CAIV siRNA on apical HCO_3^- permeability. BCECF-loaded endothelial cells were perfused in a two-sided chamber. Where indicated, the apical Ringer solution was changed from bicarbonate-rich to low-bicarbonate Ringer solution to determine the maximal rate of acidification. (**A**) This was performed twice in the absence and then in the presence of 10 μM benzolamide on the apical side. Bar graph shows mean rates and SD (n = 12 filter [Anodiscs; Whatman]). (**B**) Representative comparisons of siControl- and CAIV-treated cells. Bar graph shows mean rates and SD (n = 10 filter [Anodiscs; Whatman]).

results suggest that CAIV is not part of a transport metabolon or other complex that facilitates HCO_3^- permeability.

A small transendothelial HCO_3^- flux in the B-to-A direction can be demonstrated across corneal endothelial cell monolayers and can be shown to be inhibited by ouabain, siRNA knockdown of the basolateral 1 Na^+/2 HCO_3^- cotransporter,[33] and ethoxyzolamide (a cell-permeable CA inhibitor).[29] To measure B-to-A HCO_3^- fluxes, cells were perfused in bicarbonate-rich Ringer solution on the basolateral side and a low bicarbonate-low pH Ringer solution on the apical side. Apical perfusion was stopped, outflow was clamped, and the change in apical bath pH was measured. Figure 6A shows that 10 μM benzolamide, apical side only, had no effect on B-to-A HCO_3^- fluxes. Similarly, Figure 6B shows that CAIV siRNA treatment had no effect on B-to-A HCO_3^- fluxes. However, Figure 6C shows that, as with HCO_3^- permeability, acetazolamide had a significant inhibitory effect on transendothelial HCO_3^- flux.

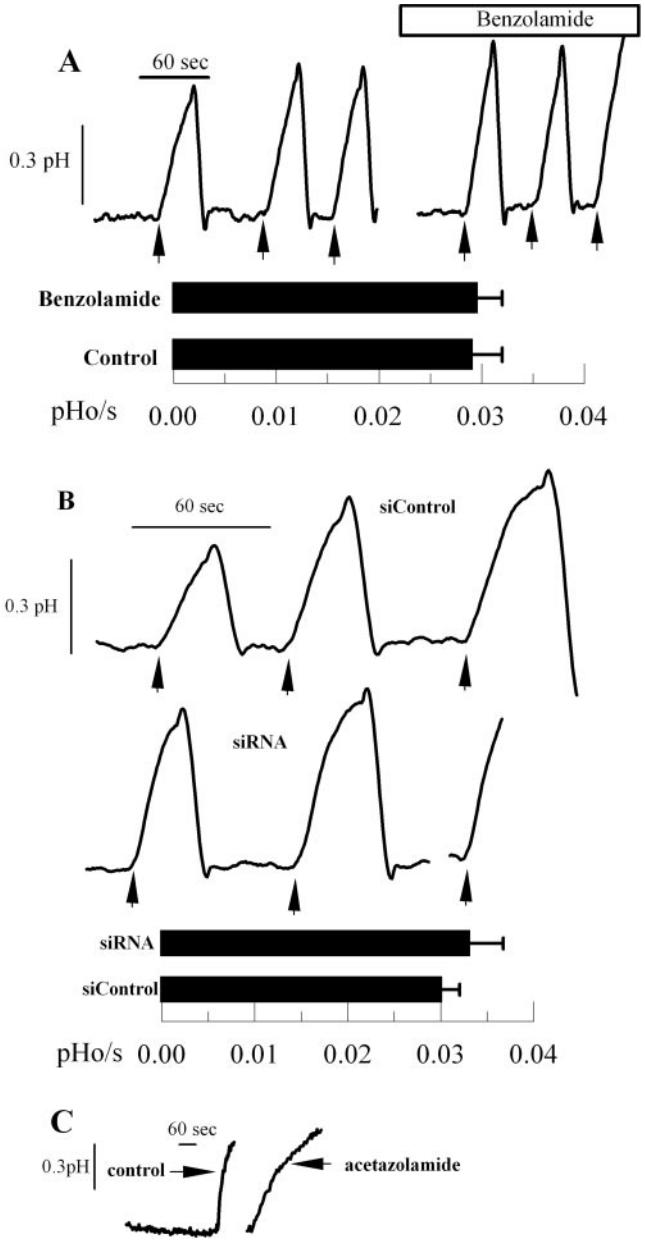

FIGURE 6. Effect of benzolamide and CAIV siRNA on B-to-A HCO_3^- flux. Endothelial cells were perfused with bicarbonate-rich Ringer solution in a two-sided chamber. The apical Ringer solution was then changed to LB Ringer solution (pH 6.5) containing 1 μM BCECF-free acid to measure apical Ringer solution pH. *Arrows* indicate when apical perfusion was stopped and apical outflow clamped. (**A**) This was performed three times in the absence and then in the presence of 10 μM benzolamide on the apical side. Bar graph shows mean rates and SD (n = 12 filter [Anodiscs; Whatman]). (**B**) Representative comparisons of siControl- and CAIV-treated cells. Bar graph shows mean rates and SD (n = 10 filter [Anodiscs; Whatman]). (**C**) Positive control; representative traces showing decreased HCO_3^- flux with 50 μM acetazolamide (n = 4) on basolateral and apical sides.

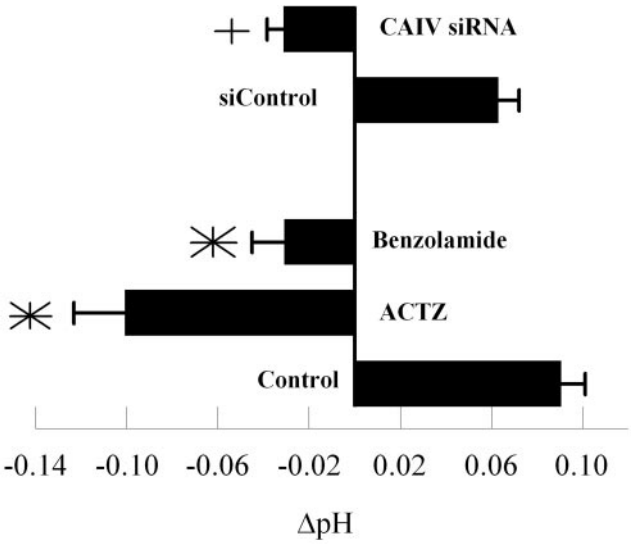

FIGURE 7. Effect of benzolamide (10 μM) and CAIV siRNA on steady state ΔpH (apical-basolateral pH) after 4 hours. ACTZ (acetazolamide 50 μM). *Significantly different from control ($P < 0.05$; $n = 6$); +significantly different from siControl. Error bars indicate SD.

Last, we examined the effects of carbonic anhydrase inhibition and CAIV knockdown on steady state ΔpH. Apical surface carbonic anhydrase activity could influence HCO_3^- fluxes, CO_2 fluxes, or apical surface buffering capacity. A reduction in ΔpH, defined as apical − basolateral pH after 4 hours, could be attributed to a reduction in net B-to-A HCO_3^- flux or a reduction in apical buffering capacity. Conversely, a reduction in net B-to-A CO_2 flux would increase ΔpH. Figure 7 shows that in control cultures, ΔpH was approximately +0.09 (apical side alkaline relative to basolateral), which is similar to what was previously reported.[33] Benzolamide, apical side only, reduced ΔpH to −0.03, significantly different from control, whereas the positive control, acetazolamide, reduced ΔpH to −0.10. In CAIV siRNA-treated cells, ΔpH was reduced to −0.03 from +0.06 pH units in siControl-treated cells. These results are consistent with reduced HCO_3^- flux or reduced buffering capacity. Given that benzolamide and CAIV siRNA did not affect apical HCO_3^- permeability (Fig. 5) or B-to-A fluxes (Fig. 6), the results are best explained by reduced buffering capacity.

DISCUSSION

Membrane-bound carbonic anhydrase activity in corneal endothelium was first demonstrated in mice[39] and rats.[15] That this was CAIV was first indicated in corneal endothelium by indirect immunohistochemistry in paraffin-embedded sections of postmortem human corneas, suggesting both basolateral and apical membrane localization.[16] Another study showed CAIV expression was present in the rabbit corneal endothelium,[17] but localization was not addressed. Here, we confirmed the expression of CAIV in bovine corneal endothelium but localized it exclusively to the apical membrane using confocal microscopy.

Although CAIs have been repeatedly shown to increase corneal thickness or to slow stromal deturgescence of swollen corneas,[1–3,19] few studies have examined mechanistic details. Ethoxyzolamide, a cell-permeant CAI, can reduce B-to-A HCO_3^- flux; however, the effects of membrane-impermeant CAIs on HCO_3^- flux were not tested.[29] Furthermore, 10 μM benzolamide or a dextran-linked CAI caused corneal swelling at approximately half the rate of cell-permeant CAIs, indicating that CAIV and CAII have additive functions and that CAIV has a role in endothelial function.[29] CAIV can facilitate apparent CO_2 flux when a CO_2 gradient is imposed across the apical membrane of bovine corneal endothelium (Fig. 4).[30] As CO_2 moves across the plasma membrane, it can be converted to HCO_3^- at the cell surface, thereby maintaining a very steep cell-to-apical surface CO_2 gradient. This process is facilitated by CAIV. Inhibition of surface CA activity slows the conversion to HCO_3^- and thereby reduces the gradient for CO_2 efflux, slowing CO_2 efflux and reducing the rate of pH_i change. On the basis of these results, the hypothesis was put forth that net CO_2 flux from cytoplasm to anterior surface and then conversion to HCO_3^- could contribute to net B-to-A HCO_3^- flux.[30] Reducing CAIV expression by siRNA had a similar effect on apparent CO_2 flux (Fig. 4), consistent with the notion that CAIV can perform this function. One difficulty with this hypothesis is that under normal physiological conditions, there is no established mechanism for net flux of CO_2 from cell-to-apical compartment as opposed to CO_2 diffusing from the cytoplasm equally in all directions. The hypothesis also predicts that the inhibition of apical CAIV activity or the knockdown of CAIV expression would slow the hydration of CO_2 at the apical surface and reduce an acidifying force. The steady state pH experiments shown in Figure 7, however, provide the opposite result, indicating that a net cell-to-apical CO_2 flux is unlikely.

Recent studies have suggested that CAIV can form a transport metabolon by binding the extracellular loops of HCO_3^- transporters.[24,40] As HCO_3^- translocates through the transporter protein from the cell to the extracellular surface, HCO_3^- can build up at the membrane, but this is dissipated by conversion to CO_2, which is facilitated by CAIV. If this existed on the endothelial apical membrane, inhibition of CAIV activity or reduction of CAIV expression would reduce apparent HCO_3^- permeability and HCO_3^- flux. The absence of an effect on permeability or flux by benzolamide or in siRNA-treated cells argues against an apical CAIV transport metabolon or other CAIV-dependent facilitation of HCO_3^- flux. One assumption in interpreting these results is that CAIV activity remains rate limiting. This arises because the pH at the apical surface is lowered from 7.5 to 6.5, slowing the hydration of CO_2 by mass action. On the other hand, carbonic anhydrases raise the reaction rate by more than 10^5 times,[20] indicating that this effect is relatively minor.

CA activity is also associated with enhancing CO_2/HCO_3^- buffering capacity.[26,27] Benzolamide has been shown to reduce cell surface buffering capacity in astrocytes[41,42] and muscle fibers.[43,44] Furthermore, we have found that cytosolic buffering capacity, measured as δpHi/s in response to an ammonium pulse, is reduced 40% in the presence of acetazolamide in cultured corneal endothelial cells (unpublished results, 2006). Taken together, the results shown in Figures 5 to 7 indicate that CAIV is not involved in facilitating HCO_3^- permeability, B-to-A HCO_3^- flux, or CO_2 flux but that it could influence apical surface buffering capacity. Confirmation of CAIV-dependent buffering will require measurement of apical surface pH changes in response to acid or base loads.

How could a reduction in apical surface buffering capacity cause corneal swelling? Does reducing apical compartment buffering cause corneal swelling? Several studies show that replacing CO_2/HCO_3^- Ringer solution with phosphate-buffered saline significantly reduces endothelial fluid transport.[1–3] Although this has been attributed to the removal of a "pump" substrate, it also significantly reduces buffering capacity. Interestingly, HCO_3^--poor Ringer solution with 50 mM added organic buffers can significantly increase endothelial transport.[45,46] One possibility is that apical buffering facilitates lactic acid efflux. Lactate/H^+ cotransport is present at the

apical membrane of corneal endothelium, and an Na-dependent lactate transport is present at the basolateral membrane[47] (this is likely to be 1 Na^+/2 HCO_3^- cotransport, in conjunction with lactate/H^+ cotransport). Thus CAIV may facilitate lactate fluxes across the apical membrane. Lactate is a potent osmolyte,[48] and the cotransporter itself is thought to couple H_2O to the transport of lactate.[49,50] Lactate fluxes can be facilitated by carbonic anhydrase activity in muscle[44,51] and glia.[42,52] Whether CA activity facilitates lactate transport across corneal endothelium remains to be tested.

In summary, CAIV is expressed in bovine corneal endothelium at the apical surface. Although inhibiting CAIV activity can reduce apparent apical CO_2 flux, this does not occur under steady state conditions. CAIV does not have a significant role in facilitating apical HCO_3^- permeability or B-to-A HCO_3^- flux. CAIV can probably contribute to apical buffering; however, further studies are needed to confirm this role and to determine whether buffering contributes to endothelial function.

Acknowledgments

The authors thank William Sly and Abdul Waheed for their kind gift of CAIV antibody.

References

1. Kuang K, Xu M, Koniarek J, Fischbarg J. Effects of ambient bicarbonate, phosphate and carbonic anhydrase inhibitors on fluid transport across rabbit endothelium. *Exp Eye Res*. 1990;50:487–493.
2. Hodson S, Miller F. The bicarbonate ion pump in the endothelium which regulates the hydration of rabbit cornea. *J Physiol*. 1976; 263:563–577.
3. Riley M, Winkler B, Czajkowski C, Peters M. The roles of bicarbonate and CO_2 in transendothelial fluid movement and control of corneal thickness. *Invest Ophthalmol Vis Sci*. 1995;36:103–112.
4. Hull DS, Green K, Boyd M, Wynn HR. Corneal endothelium bicarbonate transport and the effect of carbonic anhydrase inhibitors on endothelial permeability and fluxes and corneal thickness. *Invest Ophthalmol Vis Sci*. 1977;16:883–892.
5. Egan CA, Hodge DO, McLaren JW, Bourne WM. Effect of dorzolamide on corneal endothelial function in normal human eyes. *Invest Ophthalmol Vis Sci*. 1998;39:23–29.
6. Giasson CJ, Nguyen TQ, Boisjoly HM, Lesk MR, Amyot M, Charest M. Dorzolamide and corneal recovery from edema in patients with glaucoma or ocular hypertension. *Am J Ophthalmol*. 2000;129: 144–150.
7. Kaminski S, Hommer A, Koyuncu D, Biowski R, Barisani T, Baumgartner I. Influence of dorzolamide on corneal thickness, endothelial cell count and corneal sensibility. *Acta Ophthalmol Scand*. 1998;76:78–79.
8. Wilkerson M, Cyrlin M, Lippa EA, et al. Four-week safety and efficacy study of dorzolamide, a novel, active topical carbonic anhydrase inhibitor. *Arch Ophthalmol*. 1993;111:1343–1350.
9. Wirtitsch MG, Findl O, Kiss B, Petternel V, Heinzl H, Drexler W. Short-term effect of dorzolamide hydrochloride on central corneal thickness in humans with cornea guttata. *Arch Ophthalmol*. 2003; 121:621–625.
10. Konowal A, Morrison J, Brown S, et al. Irreversible corneal decompensation in patients treated with tropical dorzolamide. *Am J Ophthalmol*. 1999;127:403–406.
11. Tanimura H, Minamoto A, Narai A, Hirayama T, Suzuki M, Mishima HK. Corneal edema in glaucoma patients after the addition of brinzolamide 1% ophthalmic suspension. *Jpn J Ophthalmol*. 2005; 49:332–333.
12. Conroy CW, Buck RH, Maren TH. The microchemical detection of carbonic anhydrase in corneal epithelia. *Exp Eye Res*. 1992;55: 637–640.
13. Holthofer H, Siegal GJ, Tarkkanen A, Tervo T. Immunocytochemical localization of carbonic anhydrase, NaK-ATPase and the bicarbonate chloride exchanger in the anterior segment of the human eye. *Acta Ophthalmol*. 1991;69:149–154.
14. Wistrand PJ, Schenholm M, Lonnerholm G. Carbonic anhydrase isoenzymes CA I and CA II in the human eye. *Invest Ophthalmol Vis Sci*. 1986;27:419–428.
15. Terashima H, Suzuki K, Kato K, Sugai N. Membrane-bound carbonic anhydrase activity in the rat corneal endothelium and retina. *Jpn J Ophthamol*. 1995;40:142–153.
16. Wolfensberger TJ, Mahieu I, Carter ND, Hollande E, Bohnke M. Membrane-bound carbonic anhydrase (CAIV) in human corneal epithelium and endothelium. *Klin Monatsbl Augenheilkd*. 1999; 214:263–265.
17. Cui W, Liu G, Liang R. Expression of carbonic anhydrase IV in rabbit corneal endothelial cells. *Chin Med J*. 2002;115:1641–1644.
18. Gottsch JD, Seitzman GD, Margulies EH, et al. Gene expression in donor corneal endothelium. *Arch Ophthalmol*. 2003;121:252–258.
19. Fischbarg J, Lim J. Role of cations, anions, and carbonic anhydrase in fluid transport across rabbit corneal endothelium. *J Physiol*. 1974;241:647–675.
20. Gutknecht J, Bisson MA, Tosteson FC. Diffusion of carbon dioxide through lipid bilayer membranes: effects of carbonic anhydrase, bicarbonate, and unstirred layers. *J Gen Physiol*. 1977;69:779–794.
21. Purkerson JM, Schwartz GJ. The role of carbonic anhydrases in renal physiology. *Kidney Int*. 2007;71:103–115.
22. Mizumori M, Meyerowitz J, Takeuchi T, et al. Epithelial carbonic anhydrases facilitate PCO_2 and pH regulation in rat duodenal mucosa. *J Physiol*. 2006;573:827–842.
23. McMurtrie HL, Cleary HJ, Alvarez BV, et al. The bicarbonate transport metabolon. *J Enzyme Inhib Med Chem*. 2004;19:231–236.
24. Sterling D, Alvarez BV, Casey JR. The extracellular component of a transport metabolon: extracellular loop 4 of the human AE1 Cl^-/HCO_3^- exchanger binds carbonic anhydrase IV. *J Biol Chem*. 2002;277:25239–25246.
25. Sterling D, Brown NJ, Supuran CT, Casey JR. The functional and physical relationship between the DRA bicarbonate transporter and carbonic anhydrase II. *Am J Physiol Cell Physiol*. 2002;283: C1522–C1529.
26. De Marchi S, Cecchin E. Severe metabolic acidosis and disturbances of calcium metabolism induced by acetazolamide in patients on haemodialysis. *Clin Sci (Lond)*. 1990;78:295–302.
27. Leaf DE, Goldfarb DS. Mechanisms of action of acetazolamide in the prophylaxis and treatment of acute mountain sickness. *J Appl Physiol*. 2007;102:1313–1322.
28. Bonanno JA, Srinivas SP, Brown M. Effect of acetazolamide on intracellular pH and bicarbonate transport on bovine corneal endothelium. *Exp Eye Res*. 1995;60:425–434.
29. Diecke FP, Wen Q, Sanchez JM, Kuang K, Fischbarg J. Immunocytochemical localization of Na^+-HCO_3^- cotransporters and carbonic anhydrase dependence of fluid transport in corneal endothelial cells. *Am J Physiol Cell Physiol*. 2004;286:C1434–C1442.
30. Bonanno J, Guan Y, Jelamskii S, Kang X. Apical and basolateral CO_2-HCO_3^- permeability in cultured bovine corneal endothelial cells. *Am J Physiol*. 1999;277:C545–C553.
31. Bonanno JA, Giasson C. Intracellular pH regulation in fresh and cultured bovine corneal endothelium, I: Na/H exchange in the absence and presence of HCO_3^-. *Invest Ophthalmol Vis Sci*. 1992;33:3058–3067.
32. Xie Q, Zhang Y, Cai Sun X, Zhai C, Bonanno JA. Expression and functional evaluation of transient receptor potential channel 4 in bovine corneal endothelial cells. *Exp Eye Res*. 2005;81:5–14.
33. Li J, Sun XC, Bonanno JA. Role of NBC1 in apical and basolateral HCO_3^- permeabilities and transendothelial HCO_3^- fluxes in bovine corneal endothelium. *Am J Physiol Cell Physiol*. 2005;288: C739–C746.
34. Zhang Y, Li J, Xie Q, Bonanno JA. Molecular expression and functional involvement of the bovine calcium-activated chloride channel 1 (bCLCA1) in apical HCO_3^- permeability of bovine corneal endothelium. *Exp Eye Res*. 2006;83:1215–1224.
35. Yang H, Mergler S, Sun X, et al. TRPC4 knockdown suppresses epidermal growth factor-induced store-operated channel activation and growth in human corneal epithelial cells. *J Biol Chem*. 2005;280:32230–32237.

36. Tan-Allen KY, Sun XC, Bonanno JA. Characterization of adenosine receptors in bovine corneal endothelium. *Exp Eye Res*. 2005;80: 687–696.
37. Bonanno JA, Yi G, Kang XJ, Srinivas SP. Reevaluation of Cl^-/HCO_3^- exchange in cultured bovine corneal endothelial cells. *Invest Ophthalmol Vis Sci*. 1998;39:2713–2722.
38. Okuyama T, Sato S, Zhu XL, Waheed A, Sly WS. Human carbonic anhydrase IV: cDNA cloning, sequence comparison, and expression in COS cell membranes. *Proc Natl Acad Sci USA*. 1992;89: 1315–1319.
39. Ridderstrale Y, Wistrand PJ, Brechue WF. Membrane-associated CA activity in the eye of CA II-deficient mouse. *Invest Ophthalmol Vis Sci*. 1994;35:2577–2584.
40. Alvarez BV, Loiselle FB, Supuran CT, Schwartz GJ, Casey JR. Direct extracellular interaction between carbonic anhydrase IV and the human NBC1 sodium/bicarbonate co-transporter. *Biochemistry*. 2003;42:12321–12329.
41. Shah GN, Ulmasov B, Waheed A, et al. Carbonic anhydrase IV and XIV knockout mice: roles of the respective carbonic anhydrases in buffering the extracellular space in brain. *Proc Natl Acad Sci USA*. 2005;102:16771–16776.
42. Svichar N, Esquenazi S, Waheed A, Sly WS, Chesler M. Functional demonstration of surface carbonic anhydrase IV activity on rat astrocytes. *Glia*. 2006;53:241–247.
43. Kaila K, Saarikoski J, Voipio J. Mechanism of action of GABA on intracellular pH and on surface pH in crayfish muscle fibres. *J Physiol*. 1990;427:241–260.
44. Saarikoski J, Kaila K. Simultaneous measurement of intracellular and extracellular carbonic anhydrase activity in intact muscle fibres. *Pflugers Arch*. 1992;421:357–363.
45. Doughty MJ, Maurice D. Bicarbonate sensitivity of rabbit corneal endothelium fluid pump in vitro. *Invest Ophthalmol Vis Sci*. 1988; 29:216–223.
46. Doughty MJ, Newlander K, Olejnik O. Effect of bicarbonate-free balanced salt solutions on fluid pump and endothelial morphology of rabbit corneas in-vitro. *J Pharm Pharmacol*. 1993;45:102–109.
47. Giasson C, Bonanno JA. Facilitated transport of lactate by rabbit corneal endothelium. *Exp Eye Res*. 1994;59:73–81.
48. Klyce SD. Stromal lactate accumulation can account for corneal oedema osmotically following epithelial hypoxia in the rabbit. *J Physiol*. 1981;321:49–64.
49. Hamann S, Kiilgaard JF, la Cour M, Prause JU, Zeuthen T. Cotransport of H^+, lactate, and H_2O in porcine retinal pigment epithelial cells. *Exp Eye Res*. 2003;76:493–504.
50. Loo DD, Wright EM, Zeuthen T. Water pumps. *J Physiol*. 2002; 542:53–60.
51. Wetzel P, Hasse A, Papadopoulos S, Voipio J, Kaila K, Gros G. Extracellular carbonic anhydrase activity facilitates lactic acid transport in rat skeletal muscle fibres. *J Physiol*. 2001;531:743–756.
52. Svichar N, Chesler M. Surface carbonic anhydrase activity on astrocytes and neurons facilitates lactate transport. *Glia*. 2003;41: 415–419.